Supplemental material of: Interplay between process zone and material heterogeneities for dynamic cracks.

Fabian Barras,[1] Philippe H. Geubelle,[2] and Jean-François Molinari[1]

[1] Civil Engineering Institute, Institute of Materials Science and Engineering, École Polytechnique Fédérale de Lausanne (EPFL), Station 18, 1015 Lausanne, Switzerland
[2] Department of Aerospace Engineering, University of Illinois at Urbana-Champaign, 306 Talbot Laboratory, 104 South Wright Street, Urbana, IL 61801, USA

To prevent confusion with the core manuscript, labels referring to figures or equations of the supplemental material are preceded by the letter "S".

PROBLEM DESCRIPTION

Numerical method

The momentum balance equation in a linear elastic material in absence of body forces can be written as

$$c_d^2\nabla(\nabla\cdot\boldsymbol{u}) - c_s^2\nabla\times(\nabla\times\boldsymbol{u}) = \frac{\partial^2\boldsymbol{u}}{\partial t^2}, \tag{S1}$$

where c_s denotes the shear wave speed and $c_d = \sqrt{\frac{2(1-\nu)}{1-2\nu}}c_s = \eta\, c_s$ the dilatational wave speed. The numerical method adopted in this work relies on a spectral boundary integral formulation of the elastodynamic relation between the traction stresses acting on the fracture plane located between two linearly elastic half space and the resulting displacements computed on the fracture plane. The steps leading to the boundary formulation of this elastodynamic equation are detailed in [1] for the *combined formulation* and in [2] for the *independent formulation*. In this manuscript, the 2D independent formulation is adopted, for which the interface tractions τ_j are related to the displacements u_j by

$$\tau_j^{\pm}(x,t) = \tau_{0,j}^{\pm}(x,t) - V_{jk}(x,t)\frac{\partial u_k^{\pm}}{\partial t}(x,t) + f_j^{\pm}(x,t), \tag{S2}$$

where the dynamic solutions along the interface for the top and bottom continua are considered separately and denoted respectively by the subscript "±". In Equation (S2), the first right-hand side (RHS) term $\tau_{0,j}^{\pm}$ accounts for the pre-existing traction stresses present along the interface in absence of any interface perturbations, i.e., in absence of any cracks (cf. Figure 1). The second RHS term represents the instantaneous response to a change in interface velocity, where V_{jk} is the diagonal matrix

$$V_{xx} = \mu/c_s,\; V_{yy} = \eta\mu/c_s, \tag{S3}$$

with μ denoting the shear modulus. The last term, $f_j^{\pm}(x,t)$, accounts for the history of interface displacements and is expressed in the spectral domain as convolution integrals

$$[f_j^{\pm}(x,t), u_j^{\pm}(x,t)] = e^{iqx}[F_j^{\pm}(q,t), U_j^{\pm}(q,t)], \tag{S4}$$

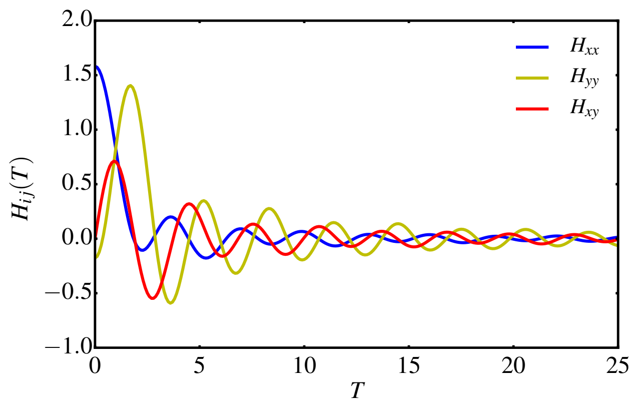

FIG. S1. Convolution kernels $H_{ij}(T)$ for $\nu = 0.35$.

with

$$\begin{aligned}
F_x^{\pm}(q,t) = &\mp \mu|q|\int_0^t H_{xx}(|q|c_s t')U_x^{\pm}(q,t-t')|q|c_s dt' \\
&+ i\mu q\int_0^t H_{xy}(|q|c_s t')U_y^{\pm}(q,t-t')|q|c_s dt' \\
&+ i(2-\eta)\mu q U_y^{\pm}(q,t)\ , \\
F_y^{\pm}(q,t) = &\mp \mu|q|\int_0^t H_{yy}(|q|c_s t')U_y^{\pm}(q,t-t')|q|c_s dt' \\
&- i\mu q\int_0^t H_{xy}(|q|c_s t')U_x^{\pm}(q,t-t')|q|c_s dt' \\
&- i(2-\eta)\mu q U_x^{\pm}(q,t)\ .
\end{aligned} \tag{S5}$$

The convolution kernels, $H_{ij}^{\pm}(T)$, whose expressions can be found in [2], are presented in Figure S1 for the material properties considered in the manuscript ($\nu = 0.35$). The spectral formulation (S2) is completed by interface conditions. For the mode-II slip-weakening interface problems of interest, these conditions imply continuity of tractions and displacements along the interface as long as the shear traction τ_x is lower than the interface strength τ^{str} defined in Equation (3). Otherwise, the fracture process breaks the continuity of displacements and the velocity $\partial u_j^{\pm}/\partial t$ of the crack faces are computed such that $\tau_x^+ = \tau_x^- = \tau^{str}$, with the value of the interface strength related to the displacement jump δ_x through the cohesive failure model described by Equation (3). Finally, the elastodynamic relations are integrated in time using an explicit time-stepping scheme

$$u_j^{\pm}(x,t+\Delta t) = u_j^{\pm}(x,t) + \frac{\partial u_j^{\pm}}{\partial t}(x,t)\Delta t, \tag{S6}$$

where the time step size defined as the fraction β of one grid spacing traveled by a shear wave: $\Delta t = \beta\ \Delta x/c_s$. In this manuscript, $\beta = 0.2$ is chosen to guarantee the stability of the solution as discussed in [2].

Material properties

Elastic material properties of Homalite have been chosen for the simulations reported in the manuscript; Young's modulus $E = 5.3$ [GPa], Poisson's ratio $\nu = 0.35$ and shear wave speed $c_s = 1263$ [m/s]. In the homogeneous segment, the interface toughness $G_c^H = 90$ [J/m^2] is defined by $\tau_c^H = 9$ [MPa] and $\delta_c = 0.02$ [mm].

EFFECT OF HETEROGENEOUS MICRO-STRUCTURE

As a complement to Figure 2, the two rupture events are also presented in Figure S2 using the same color code as in Figures 4b-c-d to highlight the heterogeneous micro-structure as well as the position of the rupture front. The growing pulse radiated in front of an accelerating shear crack [3, 4] is also clearly visible in Figure S2 as it causes early micro-cracks nucleation in the weaker areas.

TRANSITION FROM HOMOGENEOUS TO HETEROGENEOUS FRACTURE

Figure S3 presents the data of Figure 4a before normalization. The increase in slip velocity Φ (Equation (5)) is used to quantify the interplay of the dynamic front with heterogeneities. Intuitively, the crack front perturbations associated with the heterogeneous micro-structure increase with the asperity size w and/or the toughness contrast. The normalization by the characteristic length scale l_{coh} (see Figure 4a) collapses this data and explains the non-monotonic behavior observed as w changes.

PROCESS ZONE SIZE IN DYNAMIC FRACTURE

When l_{coh} becomes small compared to other characteristic dimension of the system, the rupture dynamics predicted by cohesive models is expected to meet the prediction of the singular LEFM theory based on the dynamic energy release rate expressed as

$$G_{dyn} = \frac{1-\nu^2}{E} A_{II}(v) K_{II}^2, \tag{S7}$$

where $A_{II}(v)$ is a universal function defined by

$$A_{II}(v) = \frac{\alpha_s v^2}{(1-\nu) D c_s^2}, \tag{S8}$$

where $\alpha_{s,d}^2 = 1 - v^2/c_{s,d}^2$, and $D = 4\alpha_d\alpha_s - (1+\alpha_s^2)^2$. As shown in [5], A_{II} equals one when $v = 0$ and grows to infinity as the crack speed approaches the Rayleigh wave speed c_R. Rice [6] showed that the size of the process zone for dynamic mode II crack moving at a speed v is expected to follow

$$l_{coh}(v) = l_{coh}(v=0)/A_{II}(v). \tag{S9}$$

Equation (S9) thus predicts a process zone contraction with increasing crack speed, as also captured in our simulations (see Figure 5).

[1] P. H. Geubelle and J. R. Rice, Journal of the Mechanics and Physics of Solids **43**, 1791 (1995).

[2] M. S. Breitenfeld and P. H. Geubelle, International Journal of Fracture **93**, 13 (1998).

[3] D. J. Andrews, Journal of Geophysical Research **81**, 5679 (1976).

[4] I. Svetlizky, D. Pino Munoz, M. Radiguet, D. S. Kammer, J.-F. Molinari, and J. Fineberg, Proceedings of the National Academy of Sciences **113**, 542 (2016).

[5] L. B. Freund, *Dynamic fracture mechanics*, Cambridge monographs on mechanics and applied mathematics (Cambridge University Press, Cambridge, 1990).

[6] J. R. Rice, in *Physics of the Earth's Interior* (Italian Physical Society and North Holland, 1980) pp. 555–649.

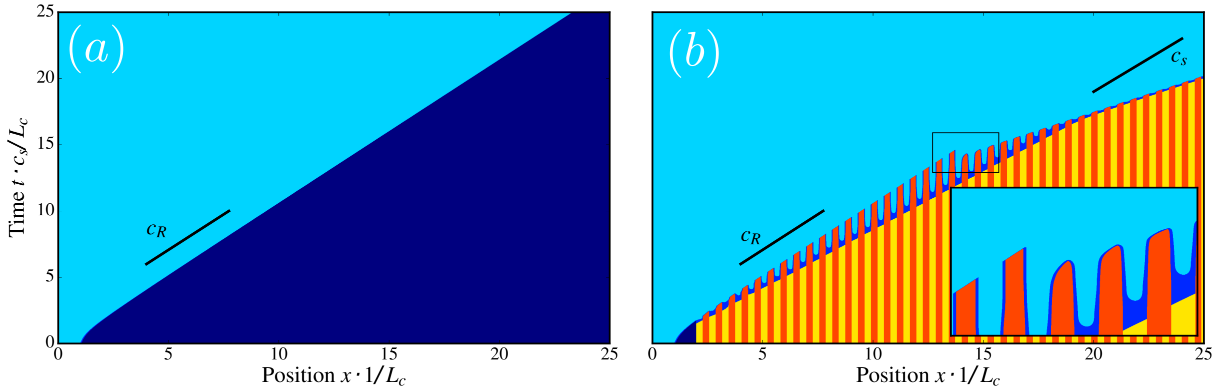

FIG. S2. Space-time diagrams of the two macroscopically equivalent dynamic fracture events described in Figures 2a and 2b of the core manuscript. The color code is the same as in Figures 4b-d.

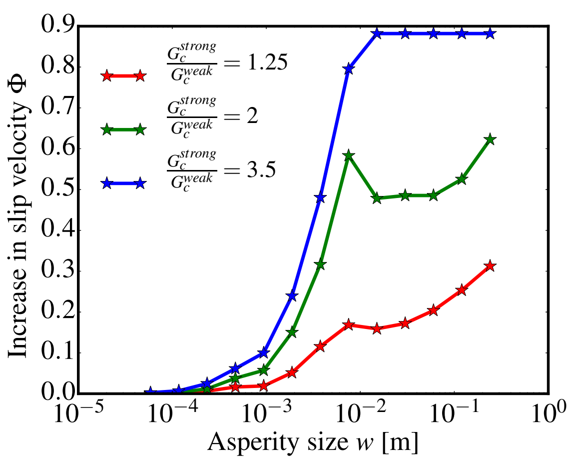

FIG. S3. Increase in slip velocity associated with the interaction of a dynamic crack growing at $v = 0.5c_s$ with an heterogeneous micro-structure of a given asperity size and toughness ratio. Figure 4a presents the same data after normalization by the process zone size.